

BROAD OMNIDIRECTIONAL REFLECTOR IN THE ONE-DIMENSIONAL TERNARY PHOTONIC CRYSTALS CONTAINING SUPERCONDUCTOR

X. Y. Dai^{1,2}, Y. J. Xiang^{2,*}, and S. C. Wen²

¹College of Electrical and Information Engineering, Hunan University, Changsha 410082, China

²Laboratory for Micro/Nano Optoelectronic Devices of Ministry of Education, School of Information Science and Engineering, Hunan University, Changsha 410082, China

Abstract—A method to enlarge the omnidirectional photonic bandgaps (PBGs) has been presented in the one-dimensional photonic crystals by sandwiching a superconductor layer between two dielectric materials to form a one-dimensional ternary periodic structure. The angle- and thickness-dependence of these PBGs have been investigated in detail, and then the thermally-tunability of these omnidirectional PBGs by controlling external temperature of the superconductor is discussed. It is shown that these omnidirectional PBGs can be extended markedly in the one-dimensional ternary photonic crystal and the gap width or the wavelength range can also be tuned by varying external temperature.

1. INTRODUCTION

Photonic crystals (PCs) are periodically distributed materials in one, two, or three spatial directions that exhibit stop bands or photonic band gaps (PBGs) [1, 2]. The electromagnetic (EM) waves with frequencies falling within PBG cannot propagate through the structure. The localized states can be created in the PBGs by introducing defects into the periodical structures. Because of their ability to control the propagation of light and the possibility of many new optical devices, PCs have been investigated intensively recently. If the PBG can reflect EM waves incident at any angle with any polarization, then an omnidirectional band gap (OBG) can be achieved

Received 20 July 2011, Accepted 9 August 2011, Scheduled 27 August 2011

* Corresponding author: Yuanjiang Xiang (Xiangyuanjiang@126.com).

with negligible loss within a specific frequency range [3–6]. In 1998, Fink et al. [3] pointed out that one-dimensional PCs (1DPCs) may have OBGs, and the general conditions for obtaining OBGs in 1DPCs are present. Since then, the OBGs in the 1DPCs have attracted great interest of many scientists [4, 7–12]. It is known that such an OBG has potential applications [13, 14], such as, omnidirectional terahertz mirrors [15], controllable switching [16], tunable polarizer [17], narrow-band filters [18], and refractometric optical sensing [19], etc.

The width of the OBGs plays an important role in the applications of 1DPC omnidirectional reflectors. However, in the one-dimensional binary photonic crystals (1DBPCs) formed by two different dielectric or metal-dielectric composites, the width of the OBGs is usually narrow, making these structures inefficient in application as total reflector mirrors. Some methods to enlarge the frequency range of OBGs have been proposed, such as increasing the contrast of dielectric functions between the PC composites [3, 4], using a chirped PC [20] or photonic heterostructure [21–23], or introducing the disorder into the periodic structures [24, 25], etc. In recent years, one-dimensional ternary photonic crystals (1DTPCs) are also put forward to obtain the extended OBGs [10, 26–31]. 1DTPCs are constituted by three material layers in a period of the lattice. Awasthi et al. [27] demonstrated that the wavelength range of OBGs can be enhanced by 108 nm when the structure was modified by sandwiching a thin layer of ZrO_2 between every two layers. When the sandwiched layer was CeF_3 , the enhancement in the range was 120 nm. Wu et al. [29] showed that the OBGs can be significant enlarged in the ternary metal-dielectric PC. Xiang et al. [26] found that the zero-effective-phase bandgap will be enlarged by sandwiching the third material between the two single-negative materials. Kong et al. [30] presented an OBG in 1D ternary plasma PC. Furthermore, some applications based on the 1DTPCs are also prospected, such as the tunable optical filter [28], and optical sensing device [10].

In the present paper, we intend to design a broad omnidirectional reflector in the 1DTPCs containing superconductor layers [32]. There is twofold purpose of adopting the superconductor. First, the ability of extending OBGs in the all-dielectric 1DTPCs is limited and the metal-dielectric 1DTPCs is inevitable to face the inherent loss issue. Such loss issue can be remedied by utilization of superconductor instead. Second, the dielectric function of the superconductor is depending on the external temperature, it is possible to design thermally-tunable omnidirectional total reflectors. Due to these two characteristics that PCs composed of superconductors and dielectric materials have started to attract research interest recently [33–37]. Our study has been carried

out as follows: Firstly, in Section 2, the theoretical models, dispersion relation and transfer matrix method in the 1DBPCs are described. Then in Section 3, we investigate systemically the properties of OBGs in this 1DBPCs, and the thickness- and temperature-dependence of the PBGs are also indicated. It is found that the wavelength range of OBGs can be enhanced by 108 nm when the structure was modified by sandwiching a superconductor layer between every two layers. The results obtained are summarized in Section 4.

2. BASIC EQUATIONS AND NUMERICAL METHOD

1DBPC $(AB)^N$ formed by alternating layers of two different dielectric materials (A and B) in the air background is depicted in the upper part of Figure 1. We assume that the thickness of the medium A (ϵ_A, μ_A) and medium B (ϵ_B, μ_B) are d_A and d_B , respectively. N is the number of periods and $d = d_A + d_B$ is the period of the unit cell in the 1DBPC. 1DTPC $(ACB)^N$ is constructed by sandwiching a thin layer of a third material C between the two layers of the binary structure periodically, as shown in the lower part of Figure 1. We assume that the medium C (ϵ_C, μ_C) is the superconductor material, and the thickness is d_C , hence the period of the unit cell in the 1DTPC is $d = d_A + d_B + d_C$.

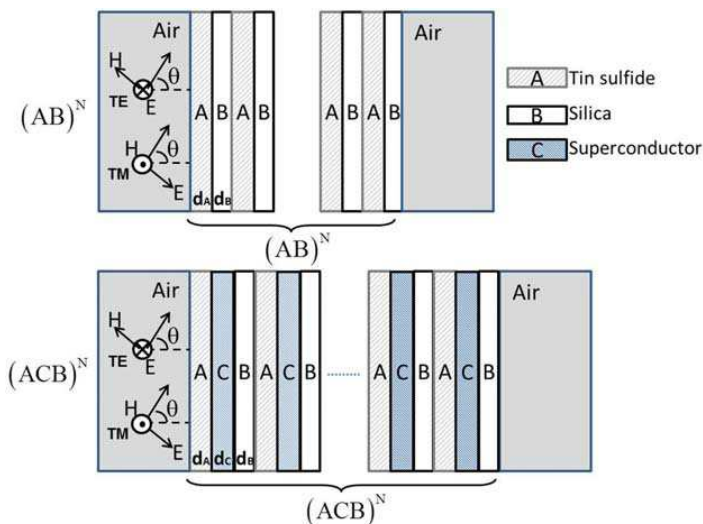


Figure 1. Schematic of a one-dimensional binary photonic crystal $(AB)^N$ and one-dimensional ternary photonic crystal $(ACB)^N$, the background is air.

In the absence of external magnetic field, we adopt the Gorter-Casimir two-fluid model [32] to describe the material properties of the superconductor. Based on the two-fluid model, the relative permittivity of lossless superconductor is given by [33, 35–37]

$$\varepsilon_C = 1 - \omega_{th}^2/\omega^2, \quad (1)$$

where ω_{th} is the threshold frequency of the bulk superconductor,

$$\omega_{th}^2 = c^2/\lambda_L^2, \quad (2)$$

c is the vacuum speed of light. λ_L is the temperature-dependent penetration depth, which is described by

$$\lambda_L = \frac{\lambda_0}{\sqrt{1 - G(T)}}, \quad (3)$$

where λ_0 is the London penetration depth at $T = 0$ K, $G(T) = (T/T_c)^p$, where T_c is the superconductor critical temperature, exponent $p = 2$ for high temperature superconductor and $p = 4$ for low temperature superconductor. In the present paper, the typical superconductor Nb is taken, and $p = 4$, $T_c = 9.2$ K, $\lambda_0 = 40$ nm are chosen in the following numerical simulations. Obviously, the superconductor has similar electromagnetic properties with the metal [29] and ε -negative metamaterial [26, 38]: when the frequency $\omega > \omega_{th}$, ε_C is positive, then the refractive-index is real, hence the superconductor behaves as a typical dielectric and the EM wave can propagate in the superconductor; however, when the frequency $\omega < \omega_{th}$, ε_C is negative, then the refractive-index becomes imaginary, hence the EM wave propagation is prohibited in the superconductor.

Figure 2(a) shows the dependence of the threshold frequency ω_{th} on the temperature T , it is clear that ω_{th} is very sensitive to the temperature, especially when the temperature T approaches to the critical temperature T_c , and ω_{th} decreases as the temperature increases. To be convenient for explanation, we also give the dependence of the threshold wavelength λ_{th} on the temperature T in Figure 2(a), it is seen that λ_{th} increases with an increase in the temperature T . When the temperature T approaches to the critical temperature T_c , λ_{th} is larger than the wavelength of visible light (390 nm–780 nm).

The temperature-sensitivity of the threshold frequency ω_{th} makes the dielectric constant of the typical superconductor Nb sensitive to the temperature T , as indicated in Figure 2(b). Here we assume that the temperature changes from 0 K to 9.1 K. At a low temperature, such as at 0 K or 3 K, the effect of the temperature T on ε_C is not very serious. When $T \leq 8$ K, ε_C is always negative in the wavelength of visible light. However, when 8 K $< T < 8.95$ K, ε_C is positive in the short

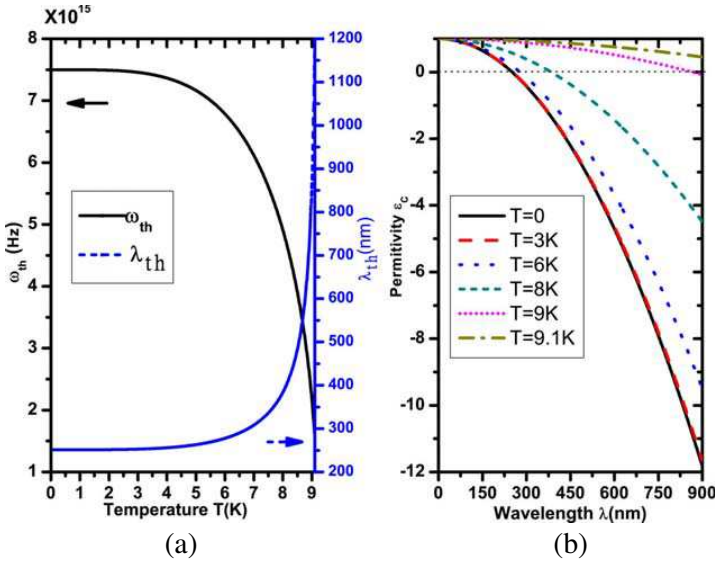


Figure 2. (a) Temperature dependence of the threshold frequency ω_{th} and threshold wavelength λ_{th} , (b) the dielectric permittivity of the typical superconductor Nb at different temperature T . The parameters are $p = 4$, $T_c = 9.2$ K, $\lambda_0 = 40$ nm.

wavelength of visible light and is negative in the long wavelength of visible light. Moreover, when the temperature T continues to increase ($T > 8.95$ K) and closes to the critical temperature T_c , ϵ_C is always positive in the wavelength of visible light.

The above analysis shows that we can tune ϵ_C by controlling external temperature, which also provides a method to achieve the tunable omnidirectional total reflector. In what follows, we will give the design scheme in detail for the broad omnidirectional reflector in 1DTPCs containing superconductor.

We use the transfer-matrix method (TMM) [39] to identify the transmittance spectra of the structure. Let a plane wave be incident from vacuum at an angle θ onto the 1DPC along $+z$ direction. Generally, the electric and magnetic fields at any two positions z and $z + \delta z$ in the same layer can be related via a transfer matrix [39],

$$M(\delta z, \omega) = \begin{pmatrix} \cos(k_{jz}\delta z) & -\frac{i}{q_{jz}} \sin(k_{jz}\delta z) \\ -iq_{jz} \sin(k_{jz}\delta z) & \cos(k_{jz}\delta z) \end{pmatrix}, \quad (4)$$

where j denote different layers, and $k_{jz} = (\omega/c)\sqrt{\epsilon_j}\sqrt{\mu_j}\sqrt{1 - \sin^2\theta/\epsilon_j\mu_j}$ are the components of the wave vector along the z axis in the medium,

$q_{jz} = \sqrt{\varepsilon_j}/\sqrt{\mu_j}\sqrt{1 - \sin^2\theta/\varepsilon_j\mu_j}$ for the TE polarization, and $q_{jz} = \sqrt{\mu_j}/\sqrt{\varepsilon_j}\sqrt{1 - \sin^2\theta/\varepsilon_j\mu_j}$ for the TM polarization, $j = A, B, C$.

For the multilayer structures, the total transfer matrix can be gotten by multiplying all individual transfer matrices of the each layer medium. Hence, the total transfer matrix connecting the field at the incident end and the exit end can be written as,

$$X(\omega) = \prod_{j=1}^{2M} M_j(\delta z, \omega) = \begin{pmatrix} x_{11}(\omega) & x_{12}(\omega) \\ x_{21}(\omega) & x_{22}(\omega) \end{pmatrix}, \quad (5)$$

Then the transmission coefficient $t(\omega)$ can be obtained from the TMM [39],

$$t(\omega) = \frac{2q_0}{(x_{11} + x_{12}q_l)q_0 + (x_{21} + x_{22}q_l)}, \quad (6)$$

and the reflection coefficient $r(\omega)$ is

$$r(\omega) = \frac{(x_{11} + x_{12}q_l)q_0 - (x_{21} + x_{22}q_l)}{(x_{11} + x_{12}q_l)q_0 + (x_{21} + x_{22}q_l)}, \quad (7)$$

Here, we assume that background material is air, hence $q_0 = q_l = \cos\theta$, $x_{k,m}(k, m = 1, 2)$ are the matrix elements of $X(\omega)$, i denotes the imaginary unit.

Moreover, for an infinite periodic structure ($M \rightarrow \infty$), based on the Bloch's theory and the boundary condition, the dispersion relation in the 1DBPC for any incident angle follows that [26, 27]

$$\begin{aligned} \cos(Kd) &= \cos(k_{Az}d_A) \cos(k_{Bz}d_B) \\ &\quad - \frac{1}{2} \left(\frac{q_{Az}}{q_{Bz}} + \frac{q_{Bz}}{q_{Az}} \right) \sin(k_{Az}d_A) \sin(k_{Bz}d_B), \end{aligned} \quad (8)$$

For the 1DTPCs, the dispersion relation can be derived as [26, 27],

$$\begin{aligned} \cos(Kd) &= \cos(k_{Az}d_A) \cos(k_{Bz}d_B) \cos(k_{Cz}d_C) \\ &\quad - \frac{1}{2} \left(\frac{q_{Az}}{q_{Bz}} + \frac{q_{Bz}}{q_{Az}} \right) \sin(k_{Az}d_A) \sin(k_{Bz}d_B) \cos(k_{Cz}d_C) \\ &\quad - \frac{1}{2} \left(\frac{q_{Az}}{q_{Cz}} + \frac{q_{Cz}}{q_{Az}} \right) \sin(k_{Az}d_A) \cos(k_{Bz}d_B) \sin(k_{Cz}d_C) \\ &\quad - \frac{1}{2} \left(\frac{q_{Bz}}{q_{Cz}} + \frac{q_{Cz}}{q_{Bz}} \right) \cos(k_{Az}d_A) \sin(k_{Bz}d_B) \sin(k_{Cz}d_C), \end{aligned} \quad (9)$$

If we assume that $d_C = 0$ in Equation (9), the dispersion relation in the 1DTPC (Equation (9)) can be recovered to the dispersion relation in the 1DBPC (Equation (8)), where K is the z component of Bloch

wave-vector. For real K , the Bloch waves are propagating; complex K indicates the presence of PBGs, where the wave propagation is inhibited.

3. RESULTS AND DISCUSSIONS

3.1. Omnidirectional Total Reflector in the 1DBPC

In the following numerical calculations, we choose tin sulfide for the dielectric medium A and silica for the dielectric medium B [5], whose refractive-indexes and thicknesses are $n_A = 2.6$, $n_B = 1.46$, $d_A = d_B = 55$ nm, respectively. A , B and C are all nonmagnetic materials, $\mu_A = \mu_B = \mu_C = 1$. The typical superconductor Nb is assumed for the material C , $p = 4$, $T_c = 9.2$ K, $\lambda_0 = 40$ nm are chosen [35], and the losses in the superconductor have been neglected. The periodical number is fixed at $N = 20$.

First, we discuss the PBG of the 1DBPCs containing two different dielectric materials A and B , the reflectance at the different incident angle θ obtained from the TMM is plotted as a function of the wavelength in Figure 3. At the normal incidence (Figure 3(a1)), the Bragg gap occurs in the wavelength of the visible light, and it is located between short wavelength $\lambda_1 = 385$ nm and long wavelength $\lambda_2 = 538$ nm, the bandwidth is $\Delta\lambda = 153$ nm. However, the band-edges

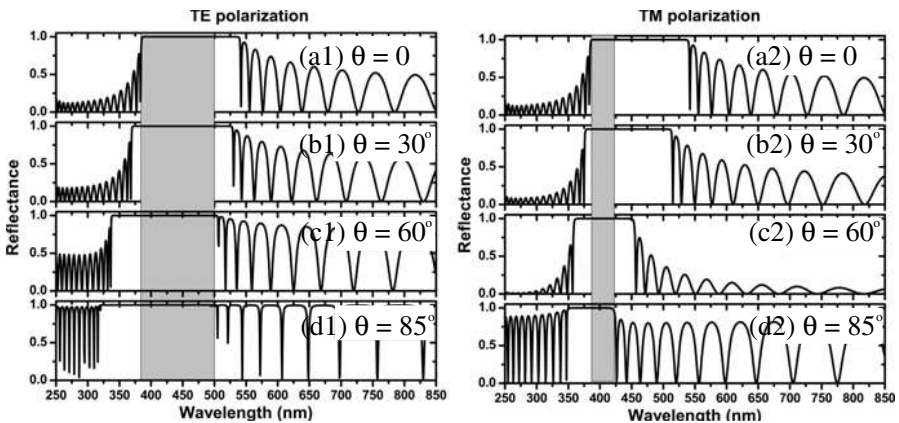


Figure 3. Reflection spectra of the one-dimensional binary photonic crystals for four different incident angle, (a1) $\theta = 0^\circ$, (b1) $\theta = 30^\circ$, (c1) $\theta = 60^\circ$, and (d1) $\theta = 85^\circ$ for TE polarization; (a2) $\theta = 0^\circ$, (b2) $\theta = 30^\circ$, (c2) $\theta = 60^\circ$, and (d2) $\theta = 85^\circ$ for TM polarization, where $d_A = d_B = 55$ nm and $T = 6$ K.

are sensitive to the incident angle θ . In order to investigate the angle-dependencies of the Bragg gap, the reflectance spectra are calculated over a number of incident angles in the range of 0° – 85° for both TE and TM polarizations. From the results of the TE polarization, as shown in Figures 3(a1)–(d1), it can be seen that the regions of the PBG are expanding with blueshift to shorter wavelength. At $\theta = 85^\circ$, the upper and lower band-edges are $\lambda_1 = 320$ nm and $\lambda_2 = 500$ nm, the bandwidth is extended to $\Delta\lambda = 180$ nm. For TE polarization, the bandwidth of PBGs in the range of 0° – 85° is $\Delta\lambda = 115$ nm. The opposite is observed for the PBG regions of TM polarization: the PBG region is shrunk with increasing angle of incidence. The upper and lower band-edges are also shifted to the shorter wavelength. At $\theta = 85^\circ$, the bandwidth is reduced to $\Delta\lambda = 70$ nm and the bandwidth of PBGs for TM polarizations in the range of 0° – 85° is $\Delta\lambda = 35$ nm.

OBG is defined by the range of overlapping of PBGs calculated for 0° and maximum possible angles of incidence for both TE and TM polarizations. In order to obtain the wavelength range of the OBGs, we have calculated the projected gap maps for both polarizations in the whole range of the angles of the incidence (0° – 90°), as indicated in Figure 4. Obviously, the bandwidth of the TE mode is larger than the TM mode; in fact, the TM mode is contained in the TE mode.

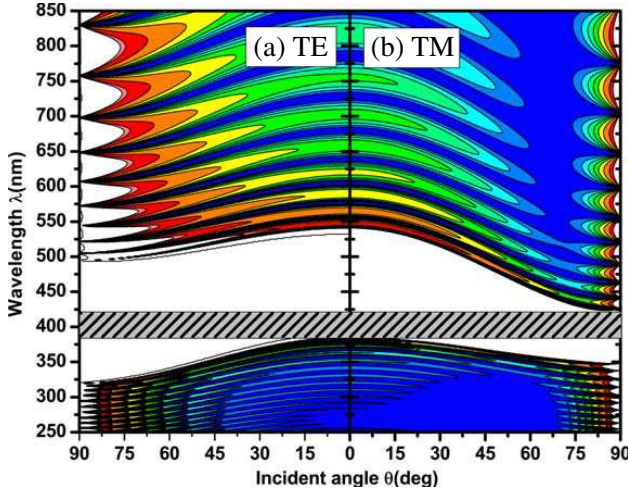


Figure 4. Projected band structures for both TE and TM polarizations of the one-dimensional binary photonic crystals, (a) TE polarization and (b) TM polarization, where $d_A = d_B = 55$ nm and $T = 6$ K.

The overlapping of the PBGs for TE and TM polarizations reveals an OBG; hence the region of OBG is determined by the bandwidth of TM polarization. The bandwidth of OBG for the 1DBPC is $\Delta\lambda = 35$ nm, it is very narrow and makes these structures inefficient in application as total reflector mirrors. Next, we will discuss how to extend the wavelength range of OBG in 1DTPC.

3.2. Extending the Wavelength Range of OBGs in the 1DTPC

The superconductor Nb has similar behavior with the metal, the permittivity ϵ_C can be positive or negative depending on the temperature and wavelength. When ϵ_C is negative, the EM wave propagation is prohibited. Therefore, the sandwiching of the superconductor Nb between the two dielectric materials A and B can suppress the propagation wave and extend the wavelength range of the PBGs. The reflectance spectra of the 1DTPC $(ACB)^N$ at different thickness d_C have been shown in Figures 5(a)–(d). It is found that PBG can be enlarged apparently when the superconductor Nb is introduced into the PC. The bandwidth is increased up to $\Delta\lambda = 210$ nm ($\lambda_1 = 382$ nm and $\lambda_2 = 592$ nm), and the lower

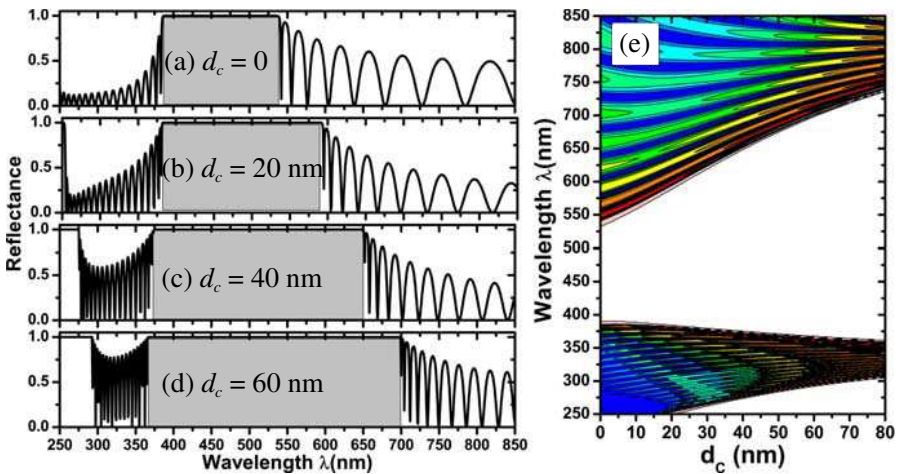


Figure 5. Reflection spectra of the one-dimensional ternary photonic crystals at normal incidence for four different thickness d_C , (a) $d_C = 0$, (b) $d_C = 20$ nm, (c) $d_C = 40$ nm, (d) $d_C = 60$ nm, (e) upper and lower band edges as a function of the thickness of the superconductor, where $d_A = d_B = 55$ nm and $T = 6$ K.

band-edge of PBG λ_1 shifts to shorter wavelength and the upper band-edge of PBG λ_2 moves to longer wavelength. The PBG can be enlarged continually as the thickness d_C increases, as shown in Figures 5(c) and (d). The bandwidth is extended to $\Delta\lambda = 330$ nm when $d_C = 60$ nm, it is more than twice compared with the bandwidth in the absent of the superconductor layers. To examine the dependence of PBGs on the thickness very carefully, we have plotted the band-edges of PBG as a function of thickness d_C . Clearly, the lower band-edge λ_1 shifts to shorter wavelength and the upper band-edge λ_2 moves to longer wavelength continually. This might be explained by the fact that the filling ratio of the superconductor increases continually with the increases of the thickness d_C .

Moreover, the wavelength range and bandwidth of the PBG are also tunable by the external temperatures due to the dependence of the superconductor (Nb) on the temperatures, which can be analyzed simply as long as we change the temperatures. The reflectance spectra at different temperatures have been plotted in Figure 6. At the low temperature ($T < 6$ K), PBGs are not sensitive to the temperature. At $T = 0$ K, the bandwidth $\Delta\lambda$ is about 337 nm. However, both the upper

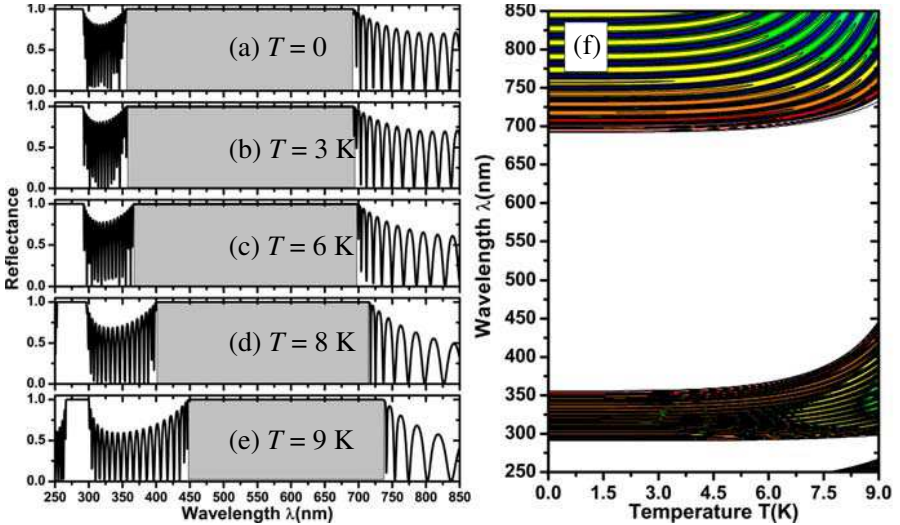


Figure 6. Reflection spectra of the one-dimensional ternary photonic crystals at normal incidence for five different temperature T , (a) $T = 0$ K, (b) $T = 3$ K, (c) $T = 6$ K, (d) $T = 8$ K, and (e) $T = 9$ K, (f) upper and lower band edges as a function of the temperature of the superconductor, where $d_A = d_B = 55$ nm and $d_C = 60$ nm.

and lower band-edges move to longer wavelength when the temperature closes to the critical temperature, meanwhile the bandwidth becomes narrower. At $T = 9$ K, the bandwidth is reduced to 285 nm. Hence, this thermally tunable PBG will provide us a pathway to design a tunable omnidirectional total reflector, optical filters and optical switching, etc.

From the above analysis, at the normal incidence, it is demonstrated that the PBG can be enlarged by introducing the superconductor into the unit cell. However, we must consider the whole range of the angle of incidence to obtain broad omnidirectional PBGs. Let's first consider the condition of the low temperature. At $T = 6$ K, the reflectance spectra of both TE and TM polarizations for a number of angles of incidence at $d_C = 60$ nm have been shown in Figure 7. For TE mode, both the short wavelength band-edge λ_1 and long wavelength band-edge λ_2 move to shorter wavelength, and the range of the overlapping wavelength for 0° to 85° is (367, 625) nm, the bandwidth is about 258 nm. However, for the TM mode, the results shown in Figures 7(a2)–(d2) show that the range of the overlapping wavelength for 0° to 85° is (367, 675) nm, the bandwidth is about 308 nm. Since the TM mode is wider than the TE mode, the region of OBG is in fact forming from the width of the TE mode in the incident angle range from 0° to 85° , as demonstrated in Figure 7. These results are the exact opposite to the results in Figure 3, where the bandwidth of the TE mode is larger than the TM mode, and the region of OBG

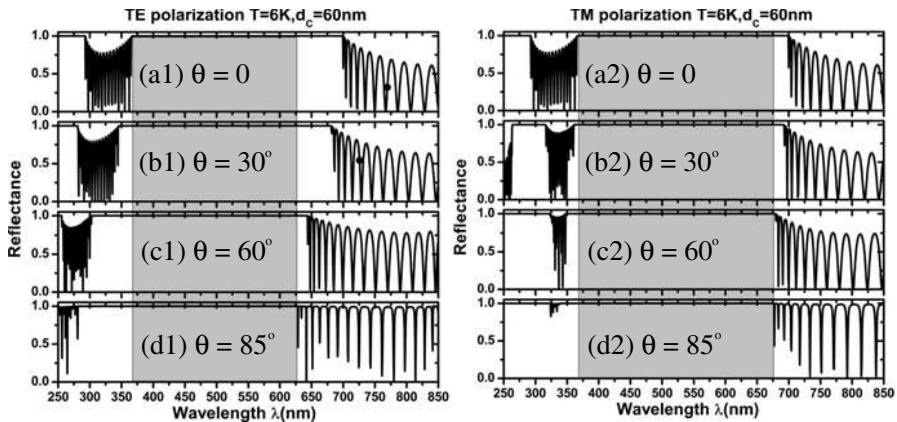


Figure 7. Reflection spectra of the one-dimensional ternary photonic crystals for four different incident angles, (a1) $\theta = 0^\circ$, (b1) $\theta = 30^\circ$, (c1) $\theta = 60^\circ$, and (d1) $\theta = 85^\circ$ for TE polarization; (a2) $\theta = 0^\circ$, (b2) $\theta = 30^\circ$, (c2) $\theta = 60^\circ$, and (d2) $\theta = 85^\circ$ for TM polarization, where $d_A = d_B = 55$ nm and $d_C = 60$ nm.

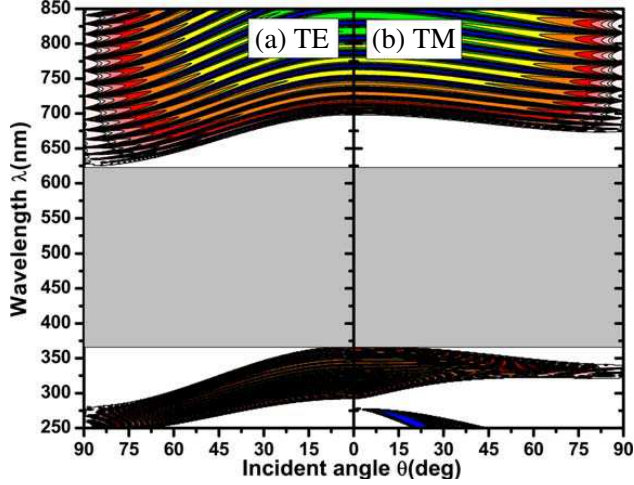


Figure 8. Projected band structures for both TE and TM polarizations of the one-dimensional ternary photonic crystals, (a) TE polarization and (b) TM polarization, where $d_A = d_B = 55$ nm, $d_C = 60$ nm and $T = 6$ K.

is determined by the bandwidth of TM polarization.

To learn the angle-dependence of the photonic band-edges for both polarizations obviously, we have plotted the projected band map for both polarizations in the whole range of the angles of incidence in Figure 8. The shaded area illustrates the wavelength regions of OBG for both polarizations. It can be seen the OBG exists and is determined by the TE mode. The OBG locates from (367, 625) nm, the omnidirectional bandwidth is about 258 nm. In comparison with the omnidirectional bandwidth in the 1DBPC, it is seen that the omnidirectional bandwidth in the 1DTPC is about seven times more than that without superconductor layer in the 1DBPC. Hence, it is a very effective method to design a broad omnidirectional OBG in the 1DTPC by sandwiching the superconductor layer between the two dielectrics in the unit cell.

In the above discussion, we just consider the effect of the superconductor layer on the omnidirectional bandwidth for the low temperature. However, in the Section 2, we have shown that at higher temperature, the permittivity ϵ_C becomes positive in the whole wavelength range of the visible light. Hence, some different behaviors can occur when the temperature T approaches to the critical temperature T_c . To specify this statement, we have plotted the reflectance spectra at $T = 9$ K for different angles of incidence in

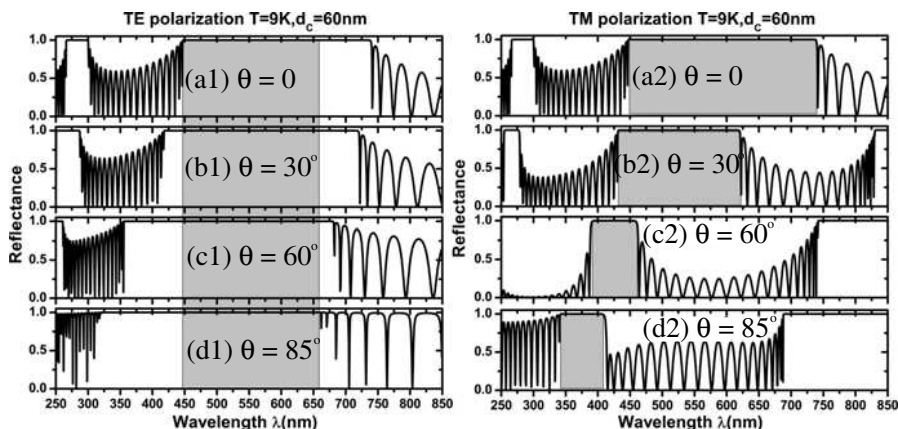


Figure 9. Reflection spectra of the one-dimensional ternary photonic crystals for four different incident angle, (a1) $\theta = 0^\circ$, (b1) $\theta = 30^\circ$, (c1) $\theta = 60^\circ$, and (d1) $\theta = 85^\circ$ for TE polarization; (a2) $\theta = 0^\circ$, (b2) $\theta = 30^\circ$, (c2) $\theta = 60^\circ$, and (d2) $\theta = 85^\circ$ for TM polarization, where $d_A = d_B = 55 \text{ nm}$, $d_C = 60 \text{ nm}$ and $T = 9 \text{ K}$.

Figure 9. For TE mode, the overlap wavelength is found in the incident angle range from angles of 0° to 85° , as shown in the shaded area in Figures 9(a1)–(d1), the wavelength range for overlapping region is (450, 660) nm, the bandwidth is about 210 nm. However, a closer look at the TM mode in Figures 9(a2)–(d2) shows that some abnormal results occur. With the increase of incidence angles, both the band-edges of short wavelength λ_1 and long wavelength λ_2 shift to short wavelength, but the movement speed of λ_2 is faster than λ_1 , the differences between the movement speeds of the two band-edges cause the shrinkage of the PBGs at larger angles of incidence. The overlap wavelength cannot be found in the incident angle range from angles of 0° to 85° for the TM mode.

The projected PBGs for both TE and TM polarizations at $T = 9 \text{ K}$ have been shown in Figure 10. Apparently, the overlapping area does not exist for both polarizations; hence OBG is absent in this case. It can be explained that the positive permittivity ϵ_C at the high temperature reduces the contrast of dielectric functions between the PC composites. Therefore, in order to obtain the omnidirectional bandwidth as large as possible, we must control the external temperature appropriately.

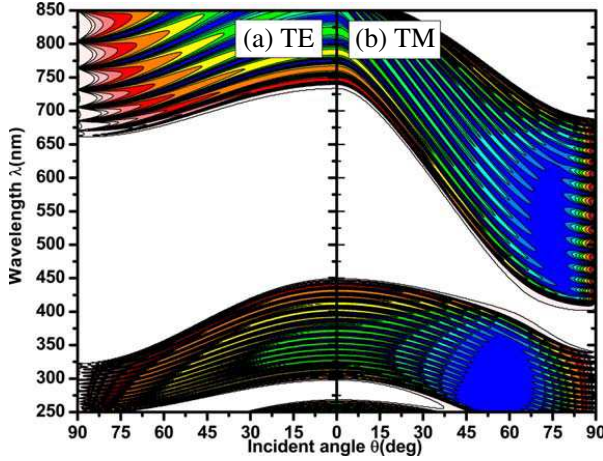


Figure 10. Projected band structures for both TE and TM polarizations of the one-dimensional ternary photonic crystals, (a) TE polarization and (b) TM polarization, where $d_A = d_B = 55$ nm, $d_C = 60$ nm and $T = 9$ K.

4. CONCLUSIONS

In summary, we have designed a new type of broad omnidirectional and thermally tunable PBGs in one-dimensional ternary photonic crystals composed of the superconductor and dielectric material. The angle- and thickness-dependence of these PBGs have been investigated. It was indicated that the gap width of these omnidirectional PBGs can be enhanced remarkably by sandwiching the superconductor layer between two dielectric materials. It manifests that the omnidirectional bandwidth in the one-dimensional ternary photonic crystals is about seven times more than that without superconductor layer in the one-dimensional binary photonic crystals. Finally, the role of the temperature in the superconductor layer on extending the PBGs was discussed. It was demonstrated that we can tune the frequency range and the width of these omnidirectional PBGs by controlling the temperature of the superconductor. It should be noted that the omnidirectional PBG disappears when the temperature is very close to the critical temperature, thus, we must control the external temperature appropriately in order to obtain the broad omnidirectional PBGs. Such an broad omnidirectional and thermally tunable PBGs will offer many prospects for omnidirectional mirrors, optical filters, polarizer, and other optical devices of optical communications in the future.

ACKNOWLEDGMENT

This work is partially supported by the National Natural Science Foundation of China (Grants 11004053, 10974049, and 61025024), the Fundamental Research Funds for the Central Universities, and the Hunan Provincial Natural Science Foundation of China (Grant 11JJB001).

REFERENCES

1. Yablonovitch, E., "Inhibited spontaneous emission in solid state physics and electronics," *Phys. Rev. Lett.*, Vol. 58, 2059–2062, 1987.
2. John, S., "Strong localization of photons in certain dielectric superlattices," *Phys. Rev. Lett.*, Vol. 58, 2486–2489, 1987.
3. Fink, Y., J. N. Winn, S. Fan, C. Chen, J. Michel, J. D. Joannopoulos, and E. L. Thomas, "A dielectric omnidirectional reflector," *Science*, Vol. 282, 1679–1682, 1998.
4. Winn, N., Y. Fink, S. Fan, and J. D. Joannopoulos, "Omnidirectional reflection from a one-dimensional photonic crystal," *Opt. Lett.*, Vol. 23, 1573–1575, 1998.
5. Deopura, M., C. K. Ullal, B. Temelkuran, and Y. Fink, "Dielectric omnidirectional visible reflector," *Opt. Lett.*, Vol. 26, 1197–1199, 2001.
6. Srivastava, R., K. B. Thapa, S. Pati, and S. P. Ojha, "Omnidirectional reflection in one dimensional photonic crystal," *Progress In Electromagnetics Research B*, Vol. 7, 133–143, 2008.
7. Li, J. S., L. Zhou, C. T. Chan, and P. Sheng, "Photonic band gap from a stack of positive and negative index materials," *Phys. Rev. Lett.*, Vol. 90, 083901, 2003.
8. Xiang, Y. J., X. Y. Dai, S. C. Wen, and D. Y. Fan, "Enlargement of zero averaged refractive index gaps in the photonic heterostructures containing negative-index materials," *Phys. Rev. E*, Vol. 76, 056604, 2007.
9. Xiang, Y. J., X. Y. Dai, S. C. Wen, and D. Y. Fan, "Independently tunable omnidirectional multichannel filters based on the fractal multilayers containing negative-index materials," *Opt. Lett.*, Vol. 33, 1255–1257, 2007.
10. Banerjee, A., "Enhanced refractometric optical sensing by using one-dimensional ternary photonic crystals," *Progress In Electromagnetics Research*, Vol. 89, 11–22, 2009.

11. Wu, C.-J. and Z.-H. Wang, "Properties of defect modes in one-dimensional photonic crystals," *Progress In Electromagnetics Research*, Vol. 103, 169–184, 2010.
12. Wu, C.-J., B.-H. Chu, and M.-T. Weng, "Analysis of optical reflection in a chirped distributed Bragg reflector," *Journal of Electromagnetic Waves and Applications*, Vol. 23, No. 1, 129–138, 2009.
13. Guida, G., A. de Lustrac, and A. Priou, "An introduction to photonic band gap (PBG) materials," *Progress In Electromagnetics Research*, Vol. 41, 1–20, 2003.
14. Ozbay, E., B. Temelkuran, and M. Bayindir, "Microwave applications of photonic crystals," *Progress In Electromagnetics Research*, Vol. 41, 185–209, 2003.
15. Krumbholz, N., K. Gerlach, F. Rutz, M. Koch, R. Piesiewicz, T. Krner, and D. Mittleman, "Omnidirectional terahertz mirrors: A key element for future terahertz communication systems," *Appl. Phys. Lett.*, Vol. 88, 202905, 2006.
16. Lu, Y. H., M. D. Huang, S. Y. Park, P. J. Kim, T. U. Nahm, Y. P. Lee, and J. Y. Rhee, "Controllable switching behavior of defect modes in one-dimensional heterostructure photonic crystals," *Jour. Appl. Phys.*, Vol. 101, 036110, 2007.
17. Awasthi, S. K., U. Malaviya, S. P. Ojha, N. K. Mishra, and B. Singh, "Design of a tunable polarizer using a one-dimensional nano sized photonic bandgap structure," *Progress In Electromagnetics Research B*, Vol. 5, 133–152, 2008.
18. Hsu, H.-T., T.-W. Chang, T.-J. Yang, B.-H. Chu, and C.-J. Wu, "Analysis of wave properties in photonic crystal narrowband filters with left-handed defect," *Journal of Electromagnetic Waves and Applications*, Vol. 24, No. 16, 2285–2298, 2010.
19. Liu, C.-C., Y.-H. Chang, and C.-J. Wu, "Refractometric optical sensing by using a multilayer reflection and transmission narrowband filter," *Journal of Electromagnetic Waves and Applications*, Vol. 24, Nos. 2–3, 293–305, 2010.
20. Wu, C.-J., B.-H. Chu, M.-T. Weng, and H.-L. Lee, "Enhancement of bandwidth in a chirped quarter-wave dielectric mirror," *Journal of Electromagnetic Waves and Applications*, Vol. 23, No. 4, 437–447, 2009.
21. Wang, X., X. Hu, Y. Li, W. Jia, C. Xu, X. Liu, and J. Zi, "Enlargement of omnidirectional total reflection frequency range in one-dimensional photonic crystals by using photonic heterostructures," *Appl. Phys. Lett.*, Vol. 80, 4291–4293, 2002.

22. Zi, J., J. Wan, and C. Zhang, "Large frequency range of negligible transmission in one-dimensional photonic quantum well structures," *Appl. Phys. Lett.*, Vol. 73, 2084–2086, 1998.
23. Srivastava, R., S. Pati, and S. P. Ojha, "Enhancement of omnidirectional reflection in photonic crystal heterostructures," *Progress In Electromagnetics Research B*, Vol. 1, 197–208, 2008.
24. Wu, C.-J., Y.-N. Rao, and W.-H. Han, "Enhancement of photonic band gap in a disordered quarter-wave dielectric photonic crystal," *Progress In Electromagnetics Research*, Vol. 100, 27–36, 2010.
25. Li, H., H. Chen, and X. Qiu, "Bandgap extension of disordered 1D binary photonic crystals," *Phys. B*, Vol. 279, 164–167, 2000.
26. Xiang, Y., X. Dai, S. Wen, Z. Tang, and D. Fan, "Extending the zero-effective-phase photonic bandgap by one-dimensional ternary photonic crystals," *Appl. Phys. B*, Vol. 103, 897–906, 2011.
27. Awasthi, S. K., U. Malaviya, and S. P. Ojha, "Enhancement of omnidirectional total-reflection wavelength range by using one-dimensional ternary photonic bandgap material," *J. Opt. Soc. Am. B*, Vol. 23, 2566–2571, 2006.
28. Awasthi, S. K. and S. P. Ojha, "Design of a tunable optical filter by using a one-dimensional ternary photonic band gap material," *Progress In Electromagnetics Research M*, Vol. 4, 117–132, 2008.
29. Wu, C.-J., Y.-H. Chung, B.-J. Syu, and T.-J. Yang, "Band gap extension in a one-dimensional ternary metal-dielectric photonic crystal," *Progress In Electromagnetics Research*, Vol. 102, 81–93, 2010.
30. Wu, X.-K., S.-B. Liu, H.-F. Zhang, C.-Z. Li, and B.-R. Bian, "Omnidirectional photonic band gap of one-dimensional ternary plasma photonic crystals," *J. Opt.*, Vol. 13, 035101, 2011.
31. Banerjee, A., "Enhanced incidence angle based spectrum tuning by using one-dimensional ternary photonic band gap structures," *Journal of Electromagnetic Waves and Applications*, Vol. 24, Nos. 8–9, 1023–1032, 2010.
32. Tinkham, M., *Introduction to Superconductivity*, McGraw-Hill, New York, 1996.
33. Lee, H. M. and J. C. Wu, "Transmittance spectra in one-dimensional superconductor-dielectric photonic crystal," *J. Appl. Phys.*, Vol. 107, 09E149, 2010.
34. Hsu, H.-T., F.-Y. Kuo, and C.-J. Wu, "Optical properties of a high-temperature superconductor operating in near zero-permittivity region," *J. Appl. Phys.*, Vol. 107, 05391, 2010.

35. Wu, C.-J., C.-L. Liu, and T.-J. Yang, "Investigation of photonic band structure in a one-dimensional superconducting photonic crystal," *J. Opt. Soc. Am. B*, Vol. 26, 2089–2094, 2009.
36. Wu, C.-J., Y.-L. Chen, and Y.-S. Tsai, "Effective surface impedance for a superconductor-semiconductor superlattice at mid-infrared frequency," *Journal of Electromagnetic Waves and Applications*, Vol. 23, Nos. 11–12, 1441–1453, 2009.
37. Wu, C.-J., C.-L. Liu, and W.-K. Kuo, "Analysis of thickness-dependent optical properties in a one-dimensional superconducting photonic crystal," *Journal of Electromagnetic Waves and Applications*, Vol. 23, Nos. 8–9, 1113–1122, 2009.
38. Xiang, Y. J., X. Y. Dai, S. C. Wen, and D. Y. Fan, "Omnidirectional and multiple-channeled high-quality filters of photonic heterostructures containing single-negative materials," *J. Opt. Soc. Am. A*, Vol. 24, A28–A32, 2007.
39. Born, M. and E. Wolf, *Principles of Optics*, 7th (expanded) edition, Cambridge University Press, Cambridge, 1999.